

# Superconductivity in S-substituted FeTe

Yoshikazu Mizuguchi<sup>1,2,3</sup>, Fumiaki Tomioka<sup>1,2</sup>, Shunsuke Tsuda<sup>1,2,4</sup>, Takahide Yamaguchi<sup>1,2</sup> and Yoshihiko Takano<sup>1,2,3</sup>

<sup>1</sup>National Institute for Materials Science, 1-2-1 Sengen, Tsukuba 305-0047

<sup>2</sup>JST, TRIP, 1-2-1 Sengen, Tsukuba 305-0047

<sup>3</sup>University of Tsukuba, 1-1-1 Tennodai, Tsukuba 305-0001

<sup>4</sup>WPI-MANA-NIMS, 1-1 Namiki, Tsukuba 305-0044

## Abstract

We have successfully synthesized a new superconducting phase of  $\text{FeTe}_{1-x}\text{S}_x$  with a PbO-type structure. It has the simplest crystal structure in iron-based superconductors. Superconducting transition temperature is about 10 K at  $x = 0.2$ . The upper critical field  $H_{c2}$  was estimated to be  $\sim 70$  T. The coherent length was calculated to be  $\sim 2.2$  nm. Because  $\text{FeTe}_{1-x}\text{S}_x$  is composed of nontoxic elements, this material is a candidate for applications and will activate more and more research on iron-based superconductor.

The discovery of superconductivity in ZrCuSiAs-structured  $\text{LaFeAsO}_{1-x}\text{F}_x$  with a transition temperature  $T_c = 26$  K [1] triggered active studies on iron-based superconductor. The  $T_c$  was raised by applying pressure ( $T_c^{\text{onset}} = 43$  K) [2] or substitution of smaller rare earth ion for the La site ( $T_c = 55$  K for  $\text{SmFeAsO}_{1-x}\text{F}_x$ ) [3]. Various iron-based superconductors, which have a structure analogous to  $\text{LaFeAsO}_{1-x}\text{F}_x$ , were discovered. Related compounds are  $\text{ThCr}_2\text{Si}_2$ -structured  $\text{Ba}_{1-x}\text{K}_x\text{Fe}_2\text{As}_2$  with  $T_c = 38$  K [4] and  $\text{Li}_{1-x}\text{FeAs}$  with  $T_c = 18$  K [5]. Recently, superconductivity at 8 K in  $\text{PbO}$ -structured  $\text{FeSe}$  is reported [6]. This compound shows a structural phase transition from tetragonal to orthorhombic around 70 K [7]. We reported a huge enhancement of  $T_c$  under high pressure ( $T_c^{\text{onset}} = 27$  K at 1.48 GPa) [8]. The  $T_c$  was also raised by the substitution of both S and Te for Se [9-11]. Density functional calculation study indicated that the stability of spin density wave is higher for  $\text{FeTe}$  than for  $\text{FeSe}$  and the doped  $\text{FeTe}$  will realize the higher  $T_c$  than that of  $\text{FeSe}$  [12].

Tetragonal  $\text{FeTe}$  has a structure very analogous to tetragonal  $\text{FeSe}$ , but does not show superconducting transition and shows a structural phase transition from tetragonal to orthorhombic around 80 K [10,13].  $\text{FeTe}$  layer, which is composed of nontoxic elements, is very advantageous for applications and activation researches on iron-based superconductors. We investigated a pressure effects of resistivity for  $\text{FeTe}_{0.92}$  up to 1.6 GPa [14]. With applying pressure, the resistivity decreased and the structural phase transition temperature shifted to a lower temperature, but superconductivity was not observed down to 2 K. These behaviors are similar to that of pressure-induced superconductivity in iron-based superconductors [15]. Thus we believed that the  $\text{FeTe}$  layer has a potential to realize superconductivity if small element is substituted to induce chemical pressures. Here we report the discovery of superconductivity in S-substituted  $\text{FeTe}_{1-x}\text{S}_x$ .

We prepared  $\text{FeTe}_{0.92}$  and  $\text{FeTe}_{1-x}\text{S}_x$  ( $x = 0.1, 0.2$ ) samples by a solid state reaction method. The samples of  $\text{FeTe}_{1-x}\text{S}_x$  were synthesized in two ways as follows; (i) The powders of Fe (99.9 %), Te (99.9 %) and S (99 %) were sealed into an evacuated quartz tube with a nominal composition of  $\text{FeTe}_{1-x}\text{S}_x$  and heated at 800 °C for 12 hours. We obtained melted samples with black surface, which contained single-crystal large grains inside. (ii) We synthesized  $\text{TeS}$  as a starting material to avoid evaporation of S at low temperatures. Te and S powders were sealed into an evacuated quartz tube with a nominal composition of  $\text{Te:S} = 1:1$  and heated at 400 °C for 12 hours. The appropriate mixture of Fe,  $\text{TeS}$ , Te powders were sealed into an evacuated quartz tube and heated at 600 °C for 12 hours. The obtained samples were reground and pressed into pellets. The

pellets were sealed into an evacuated quartz tube again and heated 600 °C for 12 hours. Finally, we obtained homogeneous black pellets. In this letter, we represent the sample names as the synthesis method, (i) or (ii), and the composition.

The obtained samples were characterized by X-ray diffraction using  $\text{CuK}\alpha$  radiation. The X-ray diffraction pattern for (ii) $\text{FeTe}_{0.8}\text{S}_{0.2}$  was refined by Rietveld refinement using Rietan2000. The ratio of Te:S was also estimated using energy dispersive X-ray spectrometer (EDX) for (i) $\text{FeTe}_{0.8}\text{S}_{0.2}$ . Temperature dependence of resistivity was measured from 300 to 2 K using a four-terminal method. Temperature dependence of magnetization was measured using a SQUID magnetometer down to 2 K.

Figure 1 shows X-ray diffraction patterns for  $\text{FeTe}_{0.92}$ , (i) $\text{FeTe}_{0.8}\text{S}_{0.2}$  and (ii) $\text{FeTe}_{0.8}\text{S}_{0.2}$ . The peaks were well indexed using space group  $P4/nmm$ .  $\text{FeTe}_{0.92}$  sample is a single phase. For (i) $\text{FeTe}_{0.8}\text{S}_{0.2}$ , weak impurity peak was observed at  $2\theta \sim 31.5^\circ$ . For (ii) $\text{FeTe}_{0.8}\text{S}_{0.2}$ , the impurity peaks were very smaller than that for (i) sample. The lattice constants are summarized in Fig.2. Both  $a$  and  $c$  axis decreased with increasing nominal S content. The  $a$  and  $c$  axis of (ii) $\text{FeTe}_{0.8}\text{S}_{0.2}$  are larger than (i) $\text{FeTe}_{0.8}\text{S}_{0.2}$ , which imply that the actual S concentration for (ii) sample is smaller than that for (i) sample.

Figure 3 shows results of Rietveld refinement for (ii) $\text{FeTe}_{0.8}\text{S}_{0.2}$  (space group  $P4/nmm$ ,  $a = 3.8123(4)$  Å,  $c = 6.2444(8)$  Å,  $V = 90.75(2)$  Å<sup>3</sup>,  $z = 0.2790(3)$ ,  $R_{\text{wp}} = 14.78$  %). The S concentration was estimated to be 5.8 % of Te. The obtained S concentration for (ii) $\text{FeTe}_{0.8}\text{S}_{0.2}$  is about 1/4 of the starting nominal composition. We also estimated the ratio of Te:S using EDX for (i) $\text{FeTe}_{0.8}\text{S}_{0.2}$ . The ratio of Te:S was estimated to be as follows; 90:10 (for the outer surface of (i) $\text{FeTe}_{0.8}\text{S}_{0.2}$ ) and 96:4 (for the inner of (i) $\text{FeTe}_{0.8}\text{S}_{0.2}$ ). The actual S concentrations estimated from Rietveld refinement and EDX are smaller than the starting nominal composition. Due to the difference of the ionic radii between S and Te, the solid solubility limit of S for the Te site may be narrow for the synthesis at ambient pressure.

Figure 4 (a) shows a temperature dependence of resistivity for  $\text{FeTe}_{0.92}$ , (i) $\text{FeTe}_{0.9}\text{S}_{0.1}$  and (i) $\text{FeTe}_{0.8}\text{S}_{0.2}$ . Fig. 4 (b) shows the enlargement of low temperatures. For  $\text{FeTe}_{0.92}$ , a strong anomaly, which corresponds to a structural phase transition, was observed around 80 K. The structural phase transition temperature shifted below 50 K for (i) $\text{FeTe}_{0.9}\text{S}_{0.1}$  and disappeared for (i) $\text{FeTe}_{0.8}\text{S}_{0.2}$ . With increasing S concentration, the normal-state resistivity decreased. At low temperature, superconducting transitions were clearly observed for the S-substituted samples. The  $T_{\text{c}}^{\text{onset}}$  was estimated by a point, which deviates from the linear temperature dependence and to be 10.0 and 10.5 K for

(i)FeTe<sub>0.9</sub>S<sub>0.1</sub> and (i)FeTe<sub>0.8</sub>S<sub>0.2</sub>. A zero resistivity was observed at 7.8 K for (i)FeTe<sub>0.8</sub>S<sub>0.2</sub>. Fig. 5 (a) shows a temperature dependence of resistivity for (i)FeTe<sub>0.8</sub>S<sub>0.2</sub> under magnetic fields up to 7 T. The estimated  $T_c^{\text{onset}}$ ,  $T_c^{\text{mid}}$  and  $T_c^{\text{zero}}$  were plotted in Fig. 5 (b) with the applied field. We estimated the upper critical field  $H_{c2}$  and the irreversible field  $H_{\text{irr}}$  by the linear extrapolation. These are the huge values of  $H_{c2}(0) = 102$  T and  $H_{\text{irr}}(0) = 56$  T. Assuming that this superconductivity is in the dirty limit,  $H_{c2}(0)$  is estimated to be  $\sim 70$  T. From the  $H_{c2}$ , the coherent length was estimated to be  $\sim 2.2$  nm using the equation of  $\xi^2 = \Phi_0 / 2\pi H_{c2}$ . Fig. 6 shows the temperature dependence of magnetization for (i)FeTe<sub>0.9</sub>S<sub>0.1</sub> and (i)FeTe<sub>0.8</sub>S<sub>0.2</sub> with zero field cooling (ZFC) and field cooling (FC) modes. The  $T_c^{\text{mag}}$  was estimated to be 8.6 K for both samples. With increasing S concentration, the shielding volume fraction was considerably enhanced. Figure 7 (a) shows the temperature dependence of resistivity for FeTe<sub>0.92</sub> and (ii)FeTe<sub>0.8</sub>S<sub>0.2</sub>, and Fig. 7 (b) shows the enlargement of low temperatures. The S substitution induced superconductivity and suppressed the structural phase transition around 80 K observed in the mother phase. The  $T_c^{\text{onset}}$  and  $T_c^{\text{zero}}$  were estimated to be 8.8 and 2.8 K.

The lattice constants clearly decreased with increasing S concentration. The S substitution corresponds to a positive chemical pressure. The decrease of resistivity and the suppression of the structural phase transition with S substitution are in good agreement with the results in pressurized FeTe. The suppression of the structural phase transition should be the key to realize superconductivity in FeTe. These results imply the possibility of superconductivity in FeTe under high pressure.

We have successfully synthesized a new superconducting phase of FeTe<sub>1-x</sub>S<sub>x</sub>. The superconductivity is now realized in FeTe layer. Up to date, superconductivity has been reported only in the FeP, FeAs or FeSe layers for iron-based superconductors. FeTe-based superconductor is advantageous for application, because it is composed of nontoxic elements. Furthermore, FeTe<sub>1-x</sub>S<sub>x</sub> has a very high  $H_{c2}$  as high as 70 T. Therefore, FeTe-based superconductor is a candidate material for applications. To raise the  $T_c$ , the search for new FeTe-based superconductors, which have a structure such as ZrCuSiAs-type, ThCr<sub>2</sub>Si<sub>2</sub>-type or multi stacking one, is required.

#### Acknowledge

This work was partly supported by Grant-in-Aid for Scientific Research (KAKENHI).

## References

- [1] Y. Kamihara, T. Watanabe, M. Hirano and H. Hosono, *J. Am. Chem. Soc.* **130** (2008) 3296.
- [2] H. Takahashi, K. Igawa, K. Arii, Y. Kamihara, M. Hirano and H. Hosono, *Nature* **453** (2008) 376.
- [3] Z. A. Ren, W. Lu, J. Yang, W. Yi, X. L. Shen, Z. C. Li, G. C. Che, X. L. Dong, L. L. Sun, F. Zhou and Z. X. Zhao, *Chin. Phys. Lett.* **25** (2008) 2215.
- [4] M. Rotter, M. Tegel and D. Johrendt, *Phys. Rev. Lett.* **101** (2008) 107006.
- [5] X. C. Wang, Q. Q. Liu, Y. X. Lv, W. B. Gao, L. X. Yang, R. C. Yu, F. Y. Li and C. Q. Jin, *cond-mat/08064688*.
- [6] F. C. Hsu, J. Y. Luo, K. W. The, T. K. Chen, T. W. Huang, P. M. Wu, Y. C. Lee, Y. L. Huang, Y. Y. Chu, D. C. Yan and M. K. Wu, *Proc. Nat. Acad. Sci.* **105** (2008) 14262.
- [7] S. Margadonna, Y. Takabayashi, M. T. McDonald, K. Kasperkiewicz, Y. Mizuguchi, Y. Takano, A. N. Fitch, E. Suard and K. Prassides, *cond-mat/08074610*. (*Chem. Commun.* 2008, DOI:10.1039/b813076k)
- [8] Y. Mizuguchi, F. Tomioka, S. Tsuda, T. Yamaguchi and Y. Takano, *Appl. Phys. Lett.* **93** (2008) 152505.
- [9] M. H. Fang, L. Spinu, B. Qian, H.M. Pham, T.J. Liu, E. K. Vehstedt, Y. Liu and Z.Q. Mao, *cond-mat/08074775*.
- [10] K. W. Yeh, T. W. Huang, Y. L. Huang, T. K. Chen, F. C. Hsu, P. M. Wu, Y. C. Lee, Y. Y. Chu, C. L. Chen, J. Y. Luo, D. C. Yan and M. K. Wu, *cond-mat/08080474*.
- [11] “Substitution effects on FeSe superconductor”, Y. Mizuguchi, F. Tomioka, S. Tsuda, T. Yamaguchi and Y. Takano, to be published.
- [12] A. Subedi, L. Zhang, D. J. Singh and M. H. Du, *Phys. Rev. B* **78** (2008) 134514.
- [13] W. Bao, Y. Qiu, Q. Huang, M. A. Green, P. Zajdel, M. R. Fitzsimmons, M. Zhernenkov, M. Fang, B. Qian, E. K. Vehstedt, J. Yang, H. M. Pham, L. Spinu, Z. Q. Mao, *cond-mat/08092058*.
- [14] Y. Mizuguchi, F. Tomioka, S. Tsuda, T. Yamaguchi and Y. Takano, *cond-mat/08105191*.
- [15] M. S. Torikachvili, S. L. Bud’ko, N. Ni, P. C. Canfield, *Phys. Rev. Lett.* **101** (2008) 057006.

#### Figure captions

Fig.1. X-ray diffraction pattern for  $\text{FeTe}_{0.92}$ , (i) $\text{FeTe}_{0.8}\text{S}_{0.2}$  and (ii) $\text{FeTe}_{0.8}\text{S}_{0.2}$ . The unidentified peaks are indicated with asterisks.

Fig.2. Lattice constants  $a$ ,  $c$  and  $V$  for all samples.

Fig.3. Results of Rietveld refinement for (ii) $\text{FeTe}_{0.8}\text{S}_{0.2}$ .

Fig.4. (a) Temperature dependence of resistivity for  $\text{FeTe}_{0.92}$  and (i) samples. Arrows in this figure indicate the maximum point of the anomaly. (b) The enlargement of low temperatures.

Fig.5. (a) Temperature dependence of resistivity for (i) $\text{FeTe}_{0.8}\text{S}_{0.2}$  under magnetic fields up to 7 T with an increment of 1 T. (b)  $H$ - $T_c$  plot. The  $T_c^{\text{onset}}$ ,  $T_c^{\text{mid}}$  and  $T_c^{\text{zero}}$  were estimated in Fig.5(a).  $H_{c2}$  and  $H_{\text{irr}}$  was estimated by the linear extrapolation.

Fig.6. Temperature dependence of magnetization for (i) $\text{FeTe}_{0.9}\text{S}_{0.1}$  and (i) $\text{FeTe}_{0.8}\text{S}_{0.2}$ .

Fig.7 (a) Temperature dependence of resistivity for  $\text{FeTe}_{0.92}$  and (ii) $\text{FeTe}_{0.8}\text{S}_{0.2}$ . (b) The enlargement of low temperatures.

Fig.1

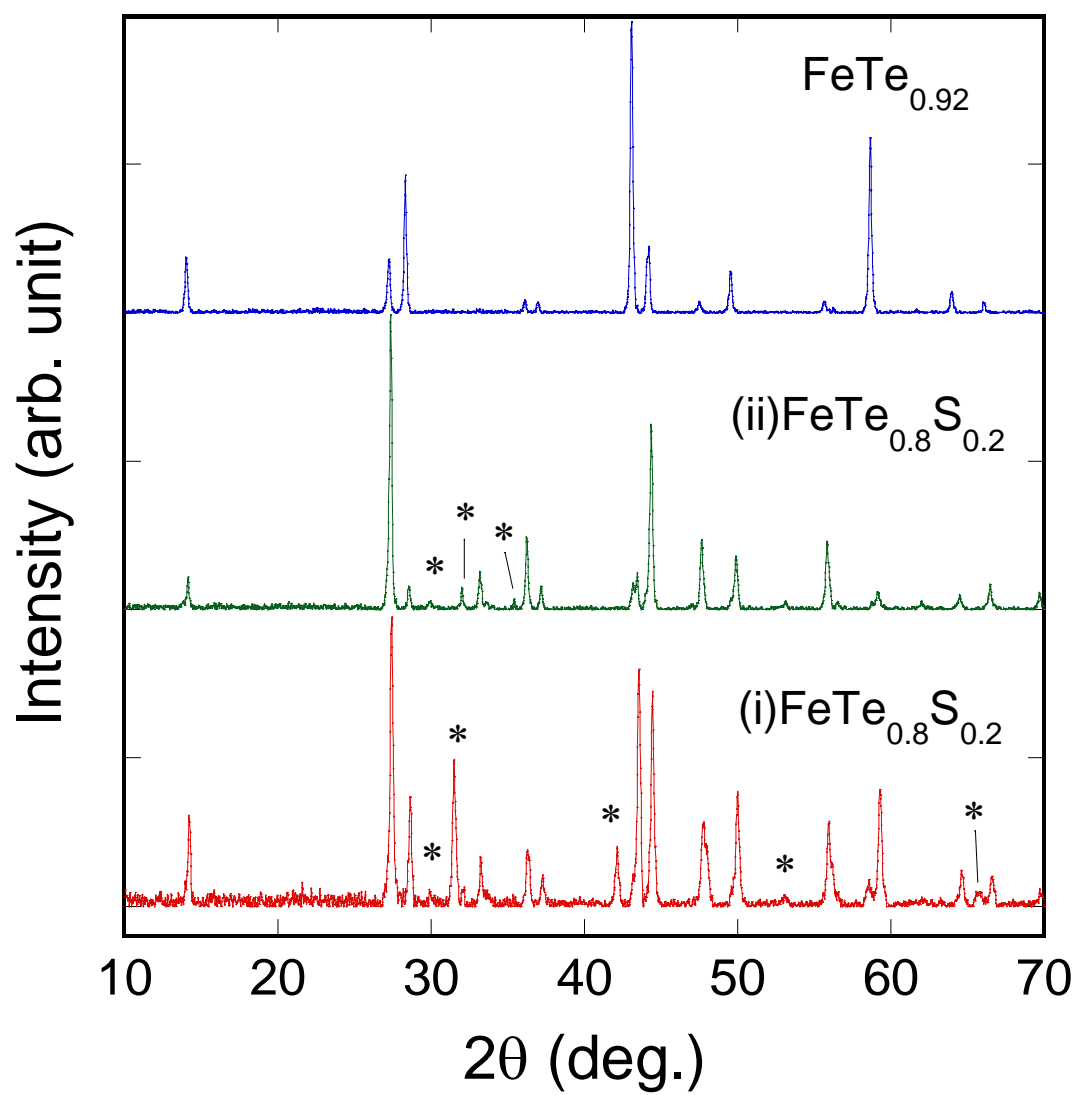


Fig.2

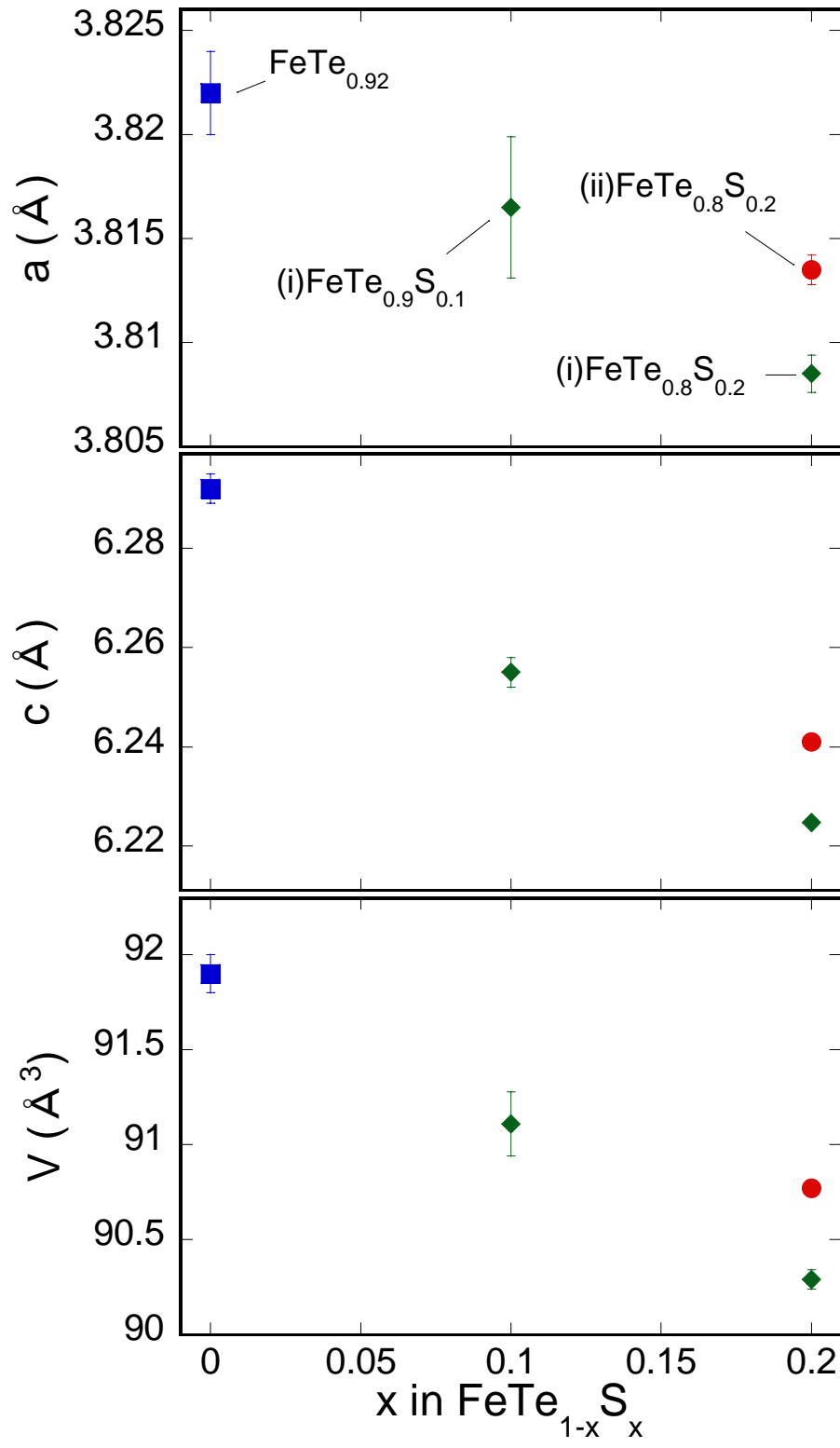




Fig.3

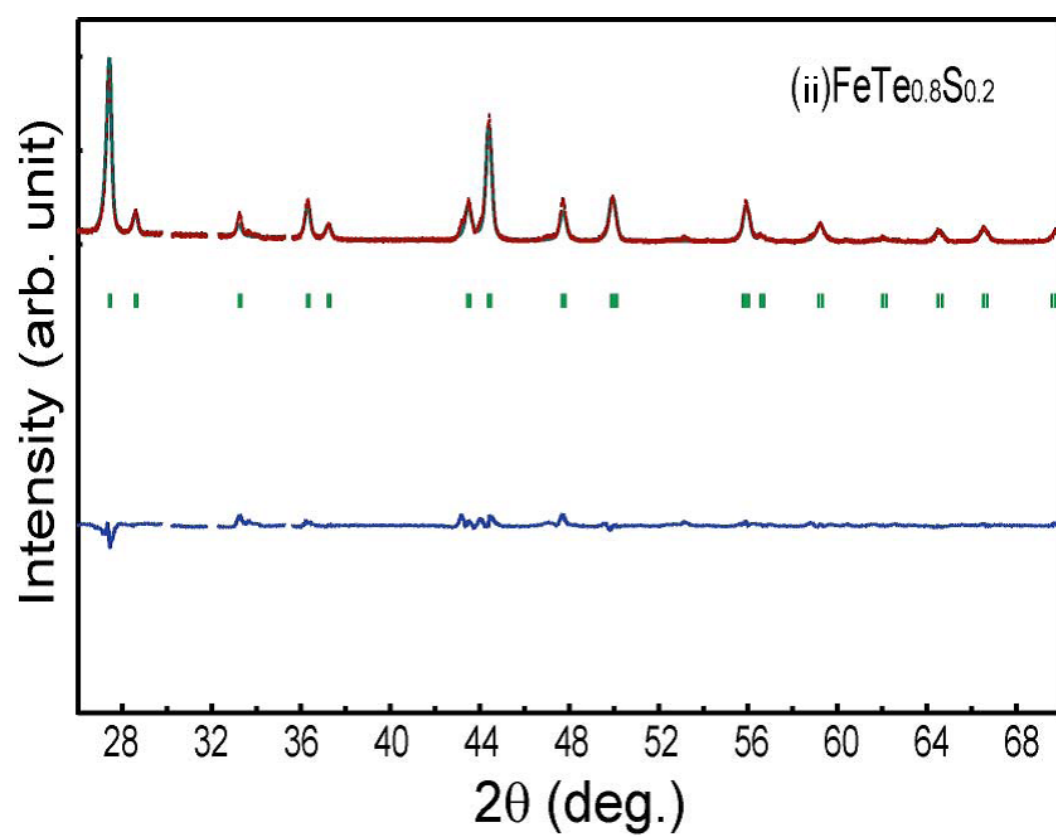
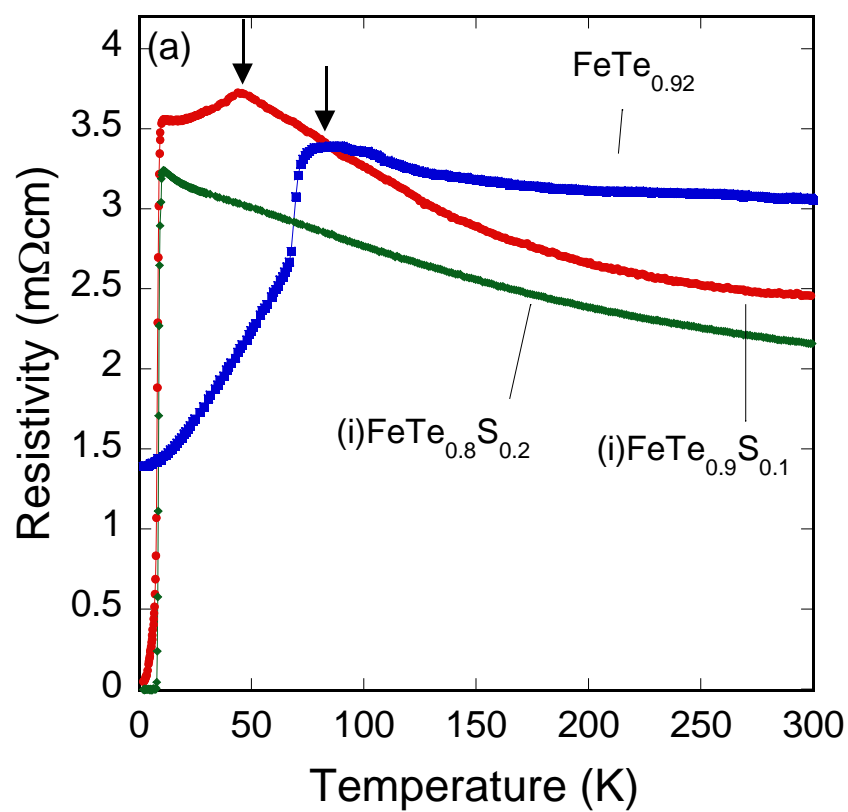


Fig.4 (a)



(b)

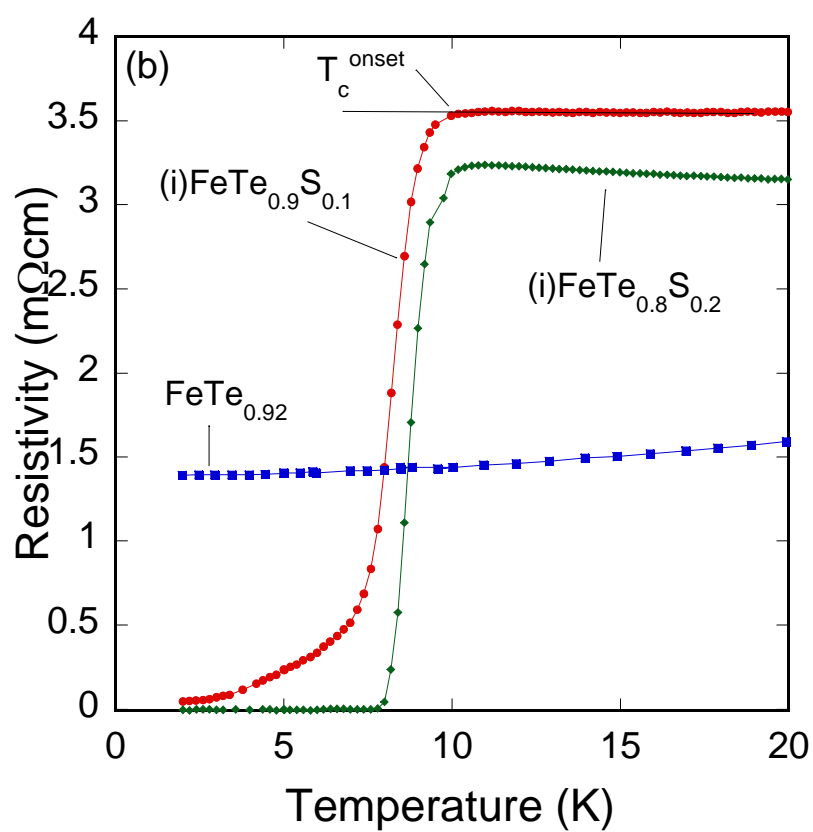


Fig.5 (a)

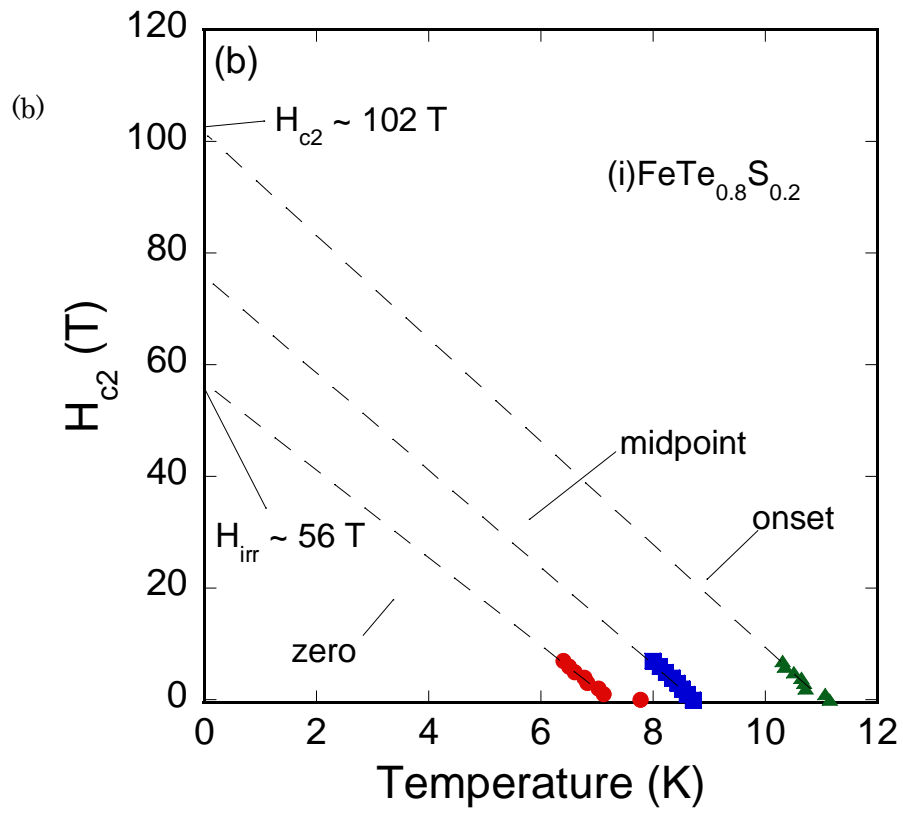
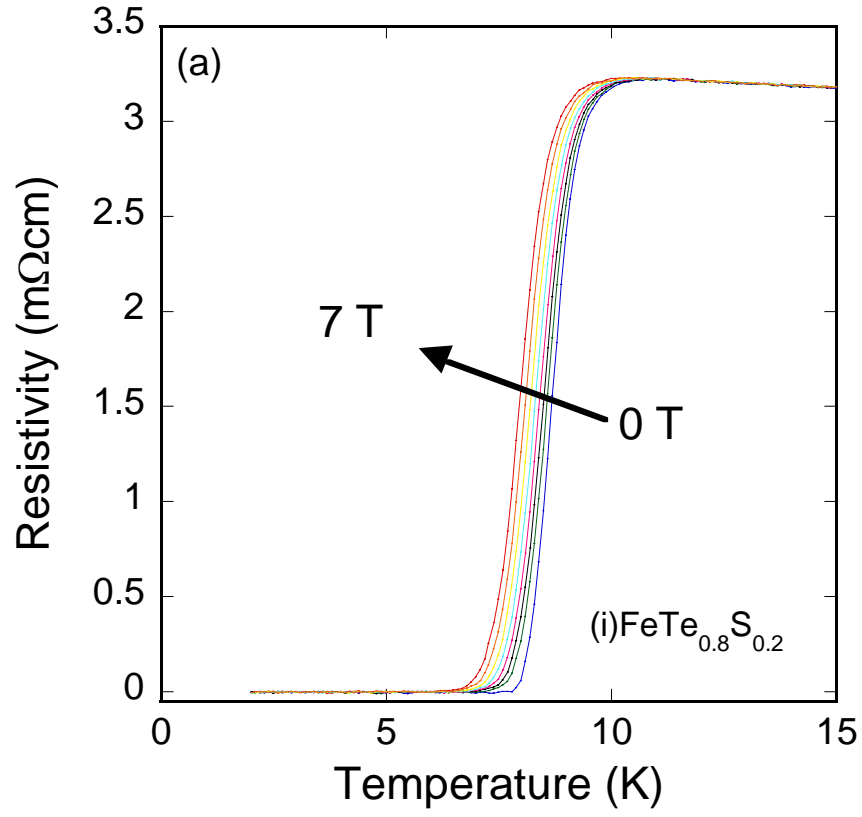


Fig.6

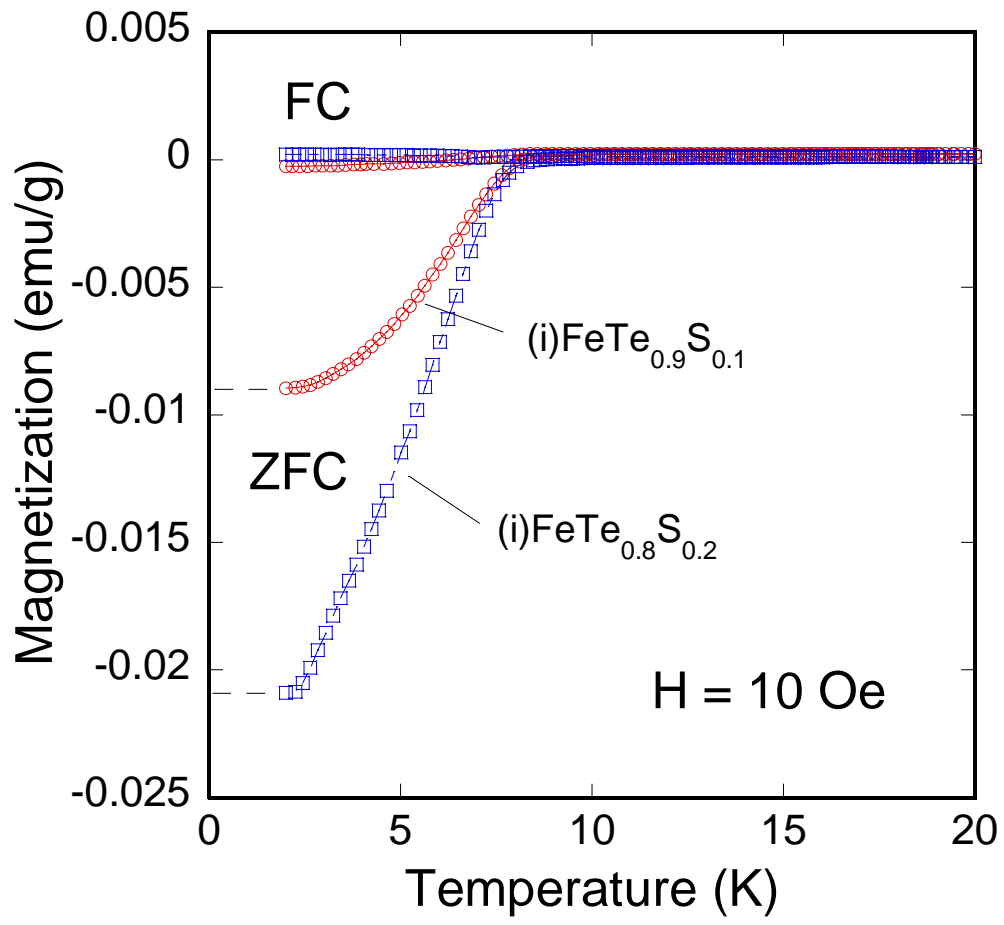


Fig.7 (a)

